10.5005/jp-journals-10009-1308
REVIEW ARTICLE

Assessment of Fetal Central Nervous System

Ritsuko K Pooh, KyongHon Pooh

ABSTRACT

Transvaginal high-resolution ultrasound and three-dimensional (3D) ultrasound has been establishing sono-embryology in the first trimester as well as neurosonography. Fetal brain is rapidly developing and changing its appearance week by week during pregnancy. The most important organ but it is quite hard to observe detailed structure of this organ by conventional transabdominal sonography. It is possible to observe the whole brain structure by magnetic resonance imaging in the post half of pregnancy, but it is difficult in the first half of gestation and transvaginal high-resolution 3D ultrasound is the most powerful modality. As for brain vascularization, main arteries and veins have been demonstrated and evaluated in various CNS conditions.

Keywords: Fetus, Central nervous system, Transvaginal scan, 3D ultrasound, Sonoembryology.

How to cite this article: Pooh RK, Pooh K. Assessment of Fetal Central Nervous System. Donald School J Ultrasound Obstet Gynecol 2013;7(4):369-384.

Source of support: Nil

Conflict of interest: None declared

INTRODUCTION

Antenatal evaluation of the fetal central nervous system (CNS) plays an important role in the field of perinatology. The brain rapidly develops *in utero* and remarkably changes its appearance from the primitive brain structure in early stage to the well-developed brain in late pregnancy.[1] Introduction of high-frequency transvaginal transducer has contributed to establishing 'sonoembryology'[2] and recent general use of transvaginal sonography in early pregnancy enabled early diagnoses of major fetal anomalies.[3] Furthermore, three-dimensional (3D) ultrasound has added accurate and objective information from early gestation till delivery, with surface anatomy, internal multidimensional analysis, volume calculation and circulatory visualization. Basic anatomical knowledge is essential, and transvaginal technique and 3D ultrasound are helpful for obtaining orientation of the brain in neuroimaging. The brain should be evaluated as a three-dimensional structure. One of reasons to make fetal neuroimaging difficult is lack of neuroanatomical knowledge. Figures 1 and 2 show basic knowledge of brain anatomy in the sagittal and coronal sections for neuroimaging diagnosis. Figure 3 shows the ventricular system.

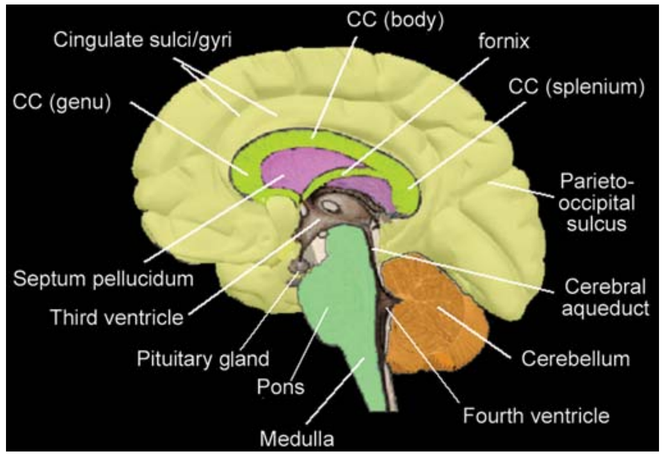

Fig. 1: Basic anatomical knowledge of sagittal cutting section of the brain. CC: corpus callosum

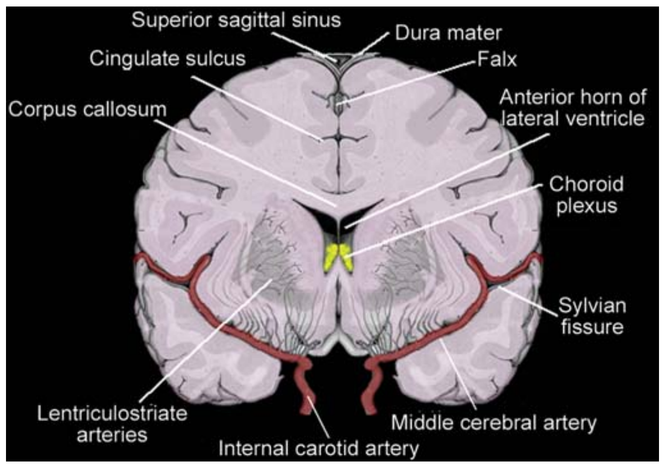

Fig. 2: Basic anatomical knowledge of coronal cutting section of the brain

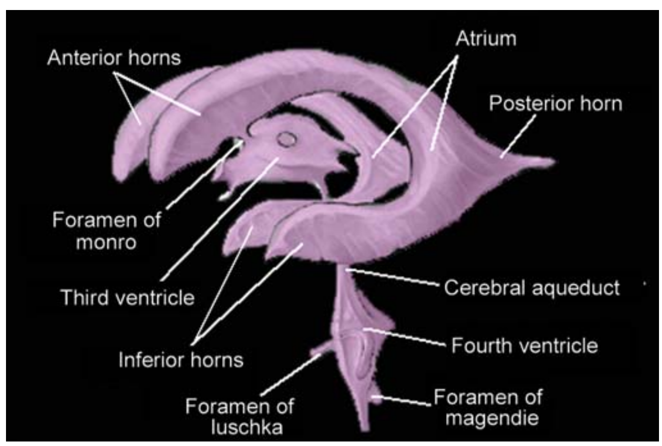

Fig. 3: Basic anatomical knowledge of ventricular system of the brain

TRANSVAGINAL APPROACH TO THE FETAL BRAIN

In the middle and late pregnancy, fetal CNS is generally evaluated through maternal abdominal wall. By transabdominal sonography, fetal brain is mostly demonstrated in transcranial axial sections. Sonographic assessment of the fetal brain in the sagittal and coronal

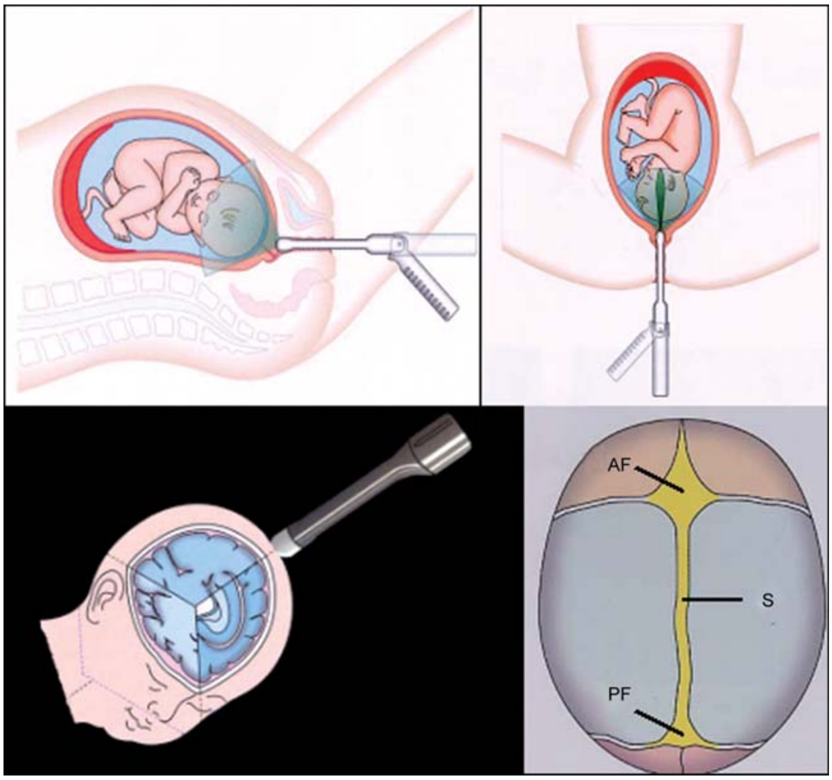

Fig. 4: Scheme of transvaginal sonography: Upper left: lateral view of vertex presenting fetus and transvaginal transducer. Upper right: frontal view of transvaginal approach. Clear imaging is possible by rotating and angle-changing of the transducer. Lower left: scheme of transfontanelle/trans-sutural approach of the fetal brain. Lower right: cranial bony structure from parietal direction. (AF: anterior fontanelle; S: sagittal suture; PF: posterior fontanelle). Those spaces are used as ultrasound windows

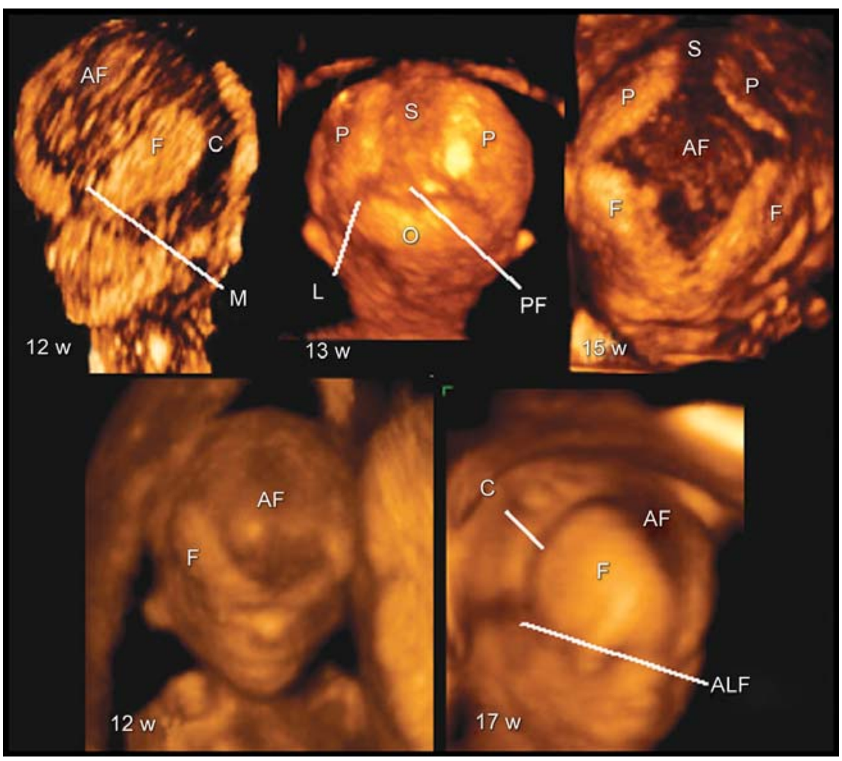

Fig. 5: Fetal cranial structure in early gestation (3D US images). Upper left: 12 weeks, from the oblique front. Upper middle: 13 weeks, from the back. Upper right: 15 weeks, from the top of head. Lower left: 12 weeks, from the front. Lower right: 17 weeks. Oblique position. Premature shape of cranial bones, sutures and fontanelles at 12 to 13 weeks change its appearance to the neonatal shape (AF: anterior fontanelle; PF: posterior fontanelle; ALF: anterolateral fontanelle; F: frontal bone; P: parietal bone; O: occipital bone; C: coronal suture; M: metopic suture; S: sagittal suture; L: lambdoid suture)

sections, requires an approach from fetal parietal direction. Transvaginal sonography of the fetal brain opened a new field in medicine, 'neurosonography'.[4] Transvaginal approach to the normal fetal brain during the second and third trimesters was introduced in the beginning of 1990s. It was the first practical application of three-dimensional central nervous system assessment by two-dimensional (2D) ultrasound.[5] Transvaginal observation of the fetal brain (Fig. 4) offers sagittal and coronal views of the brain from fetal parietal direction[6-10] through the fontanelles and/or the sagittal suture as ultrasound windows. Serial oblique sections[4] via the same ultrasound window reveal the intracranial morphology in detail. This method has contributed to the prenatal sonographic assessment of congenital CNS anomalies and acquired brain damage *in utero*, especially when compared with conventional transabdominal method.

THREE-DIMENSIONAL TRANSVAGINAL SONOGRAPHY

Introduction of 3D ultrasound in obstetrics[11-13] has produced not only objective imaging of fetal superficial structure but also a combination of both transvaginal sonography and 3D ultrasound may be a great diagnostic tool for evaluation of three-dimensional structure of fetal CNS.[14-20] 3D transvaginal sonography demonstrates bony structure such as cranial os (Fig. 5) and vertebrae (Fig. 6), multiplanar analysis of inside morphology from early till late pregnancy

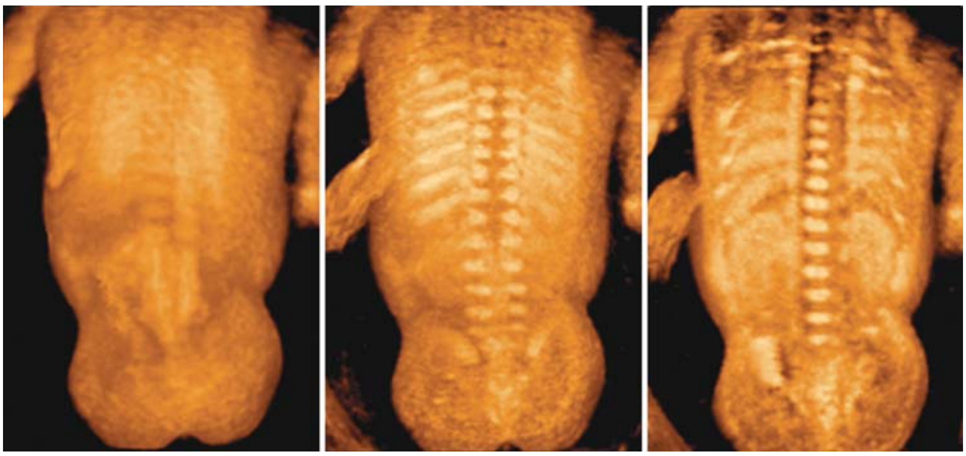

Fig. 6: Fetal back and vertebral structure of 16-week normal fetus (3D US images). Left: fetal back surface. Middle: inside of the fetus. Lamina of vertebra and ribs are clearly observed. Right: vertebral bodies and intervertebral disk spaces are seen

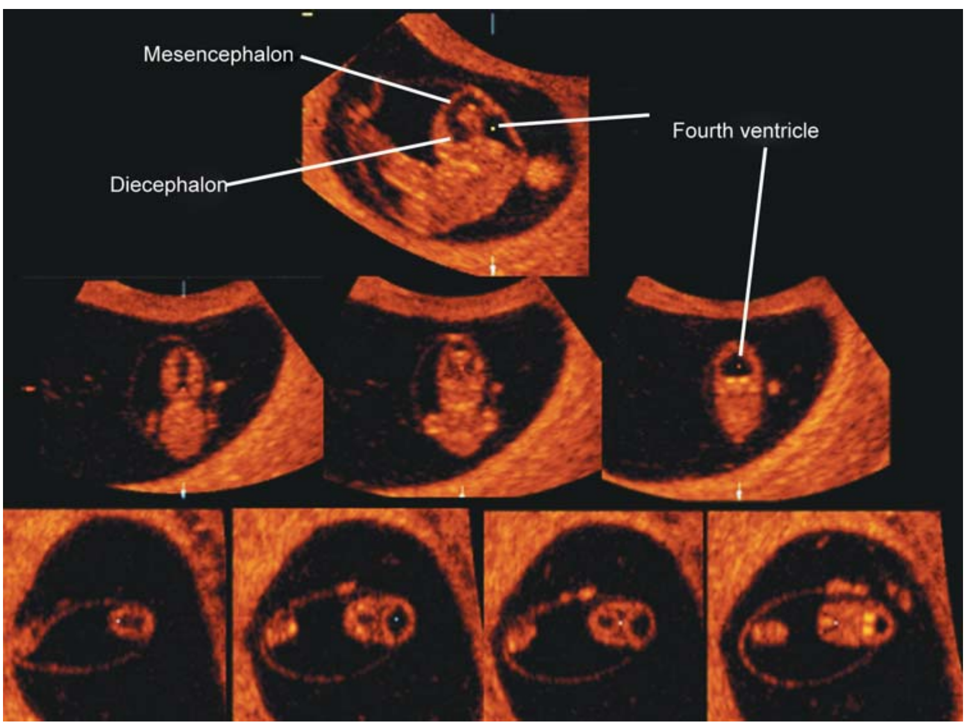

Fig. 7: Normal intracranial structure at 8 weeks of gestation in parallel cutting slices of three orthogonal views. Sagittal, coronal, axial sections from above. Premature sonolucent ventricular system is visible

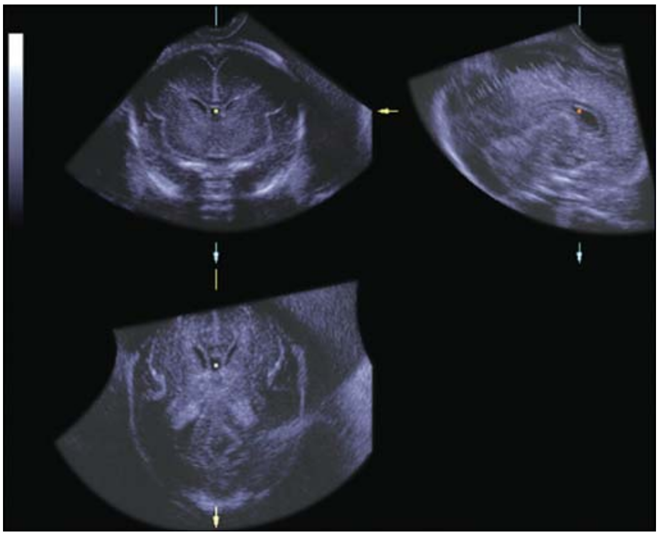

Fig. 8: 3D multiplanar image analysis. Three orthogonal views are useful to obtain orientation of the brain structure. The raw 3D volume dataset can be saved quickly. Saved data can be reviewed on ultrasound devise, and extracted images can be sent for consultation. Off-line image analysis can be done easily and repeatedly

(Figs 7 to 9), sonoangiography (Fig. 10), and volume extraction and calculation of target organ, i.e. lateral ventricle and/or choroids plexus (Fig. 11). Some recent papers described high reliability of 3D fetal brain volume measurements.[21,22]

HYDROCEPHALUS AND VENTRICULOMEGALY

Hydrocephalus and ventriculomegaly are often used interchangeably to describe dilatation of the fetal lateral ventricles. However, they should be distinguished from each other to assess the enlargement of ventricles. Hydrocephalus is a dilatation of the lateral ventricles resulted from increased amount of cerebrospinal fluid and increased intracranial pressure, while ventriculomegaly is a dilatation of lateral ventricles with nonincreased intracranial pressure, due to hypoplastic cerebrum or other intracerebral abnormalities such as agenesis of the corpus callosum. In sonographic imaging, these two intracranial conditions can be differentiated by visualization of subarachnoid space and appearance of choroid plexus. The transvaginal oblique and coronal images demonstrate the obliterated subarachnoid space and the dangling choroid plexus in the case of hydrocephalus (Figs 12 and 13). In contrast, the subarachnoid space and choroid plexus are well preserved in the case of ventriculomegaly[9] (Fig. 14). It is difficult to evaluate obliterated subarachnoid space in the axial section. Therefore, it is suggested that the evaluation of fetuses with enlarged ventricles may be evaluated by parasagittal and coronal views taken by transvaginal way. Furthermore, intracranial venous blood flow may be related to increased intracranial pressure. In normal fetuses, blood flow waveforms of dural sinuses, such as superior sagittal sinus, vein of Galen and straight sinus have pulsatile pattern[23] (Fig. 15). However, in cases with progressive hydrocephalus, normal pulsation disappears and blood flow waveforms become flat pattern[23] (Fig. 16). In cases with progressive hydrocephalus, there may be seven stages of progression (Fig. 17); (i) increased fluid collection of lateral ventricles, (ii) increased intracranial pressure, (iii) dangling choroids plexus, (iv) disappearance of subarachnoid space, (v) excessive extension of the dura and SSS, (vi) disappearance of venous pulsation, and (vii) enlarged skull.

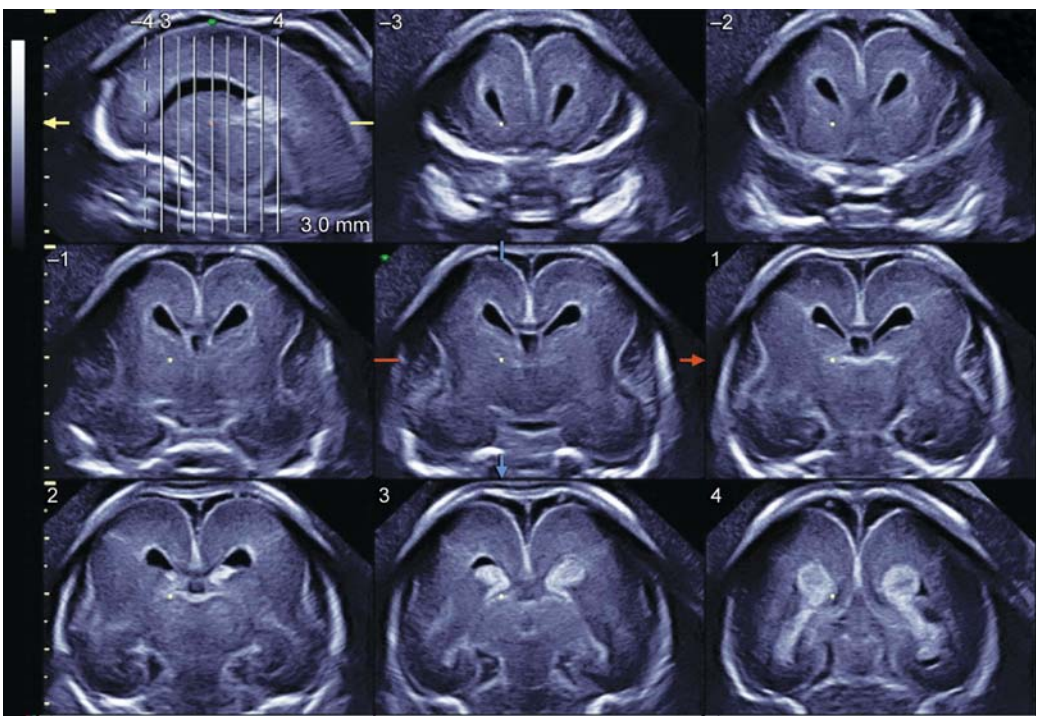

Fig. 9: Normal intracranial structure at 20 weeks of gestation in parallel cutting coronal sections

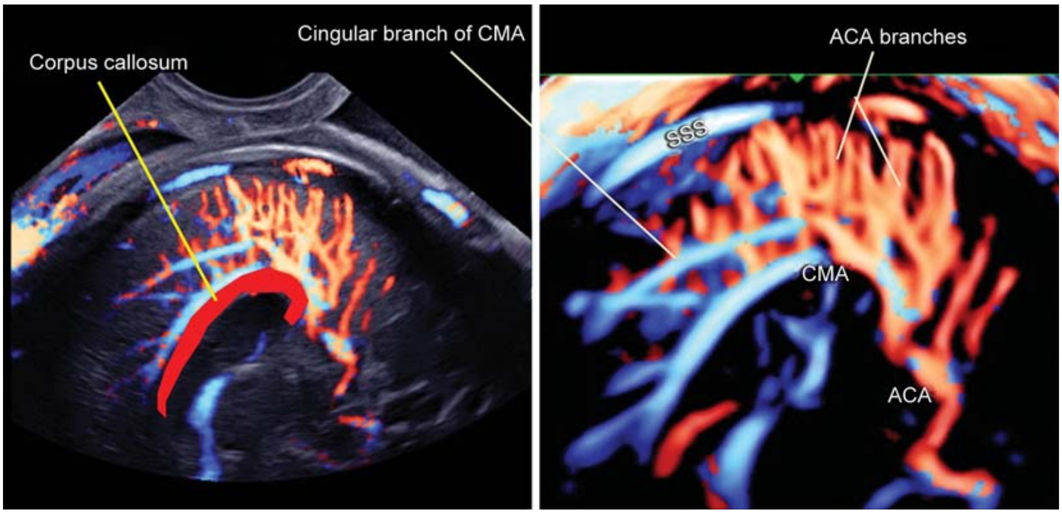

Fig. 10: Bidirectional power Doppler 2D image (left) and 3D reconstructed image (right) in the sagittal section of 24-weeker normal brain. CMA: callosomarginal artery; ACA: anterior cerebral artery; SSS: superior sagittal sinus

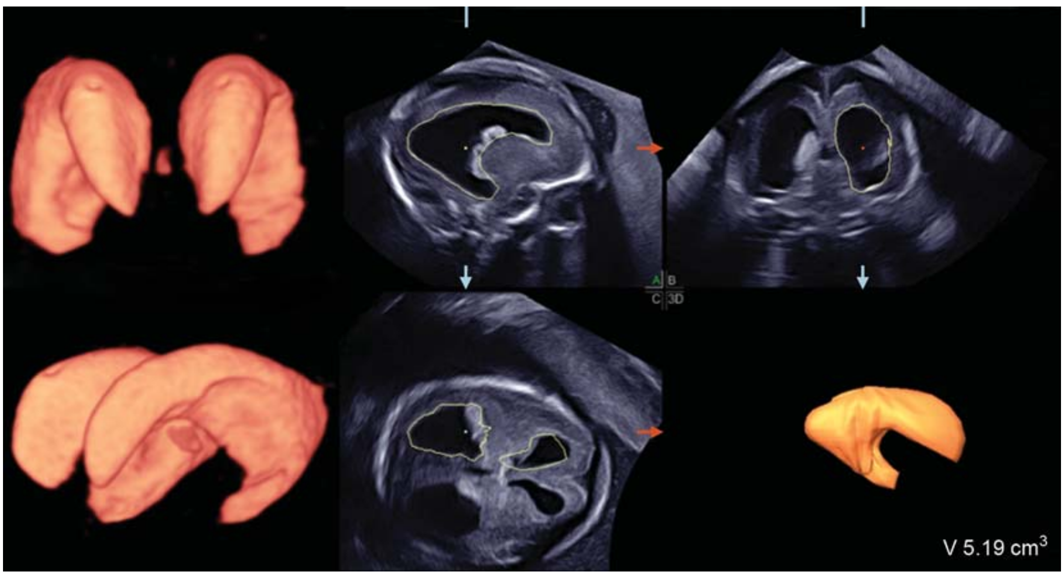

Fig. 11: 3D volume extraction of the lateral ventricles by inversion mode (left) and volumetric analysis of lateral ventricle (right) in a ventriculomegaly case at 19 weeks

TRANSVAGINAL ASSESSMENT OF CONGENITAL CNS ANOMALIES

Neurulation Disorders (Cranium Bifidum and Spina Bifida)

Cranium Bifidum

The calvarial ossification started at 10 weeks of gestation and the hyperechogenic skull appears in sonographic image by 11 weeks in normal pregnancy. Cranium bifidum is classified into four types of encephaloschisis (including anencephaly and exencephaly), meningocele, encephalomeningocele, encephalocystocele and cranium bifidum occulutum. Encephalocele occurs in the occipital region in 70 to 80%. Many reported remarkable reduction of prevalence of NTDs after using folic acid supplementation and fortification,[24-27] although some reported no decline of anencephaly rate.[28] Acrania, exencephaly (Fig. 18) and anencephaly (Fig. 19), caused by disorder of neurulation, are not independent anomalies. It is considered that dysraphia (absent cranial vault, acrania) occurs in very early stage and disintegration of the exposed brain (exencephaly) during the fetal period results in anencephaly.[29]

Spina Bifida

Spinal dysraphism is the most common abnormality of the central nervous system. Prevalence rate has been declined due to folic acid supplementation and fortification. Spina bifida aperta, manifest form of spina bifida, is classified into four types: meningocele, myelomeningocele, myelocystocele, myeloschisis. Approximately 10 to 15% of spinal dysraphic defects are closed and normal skin covers

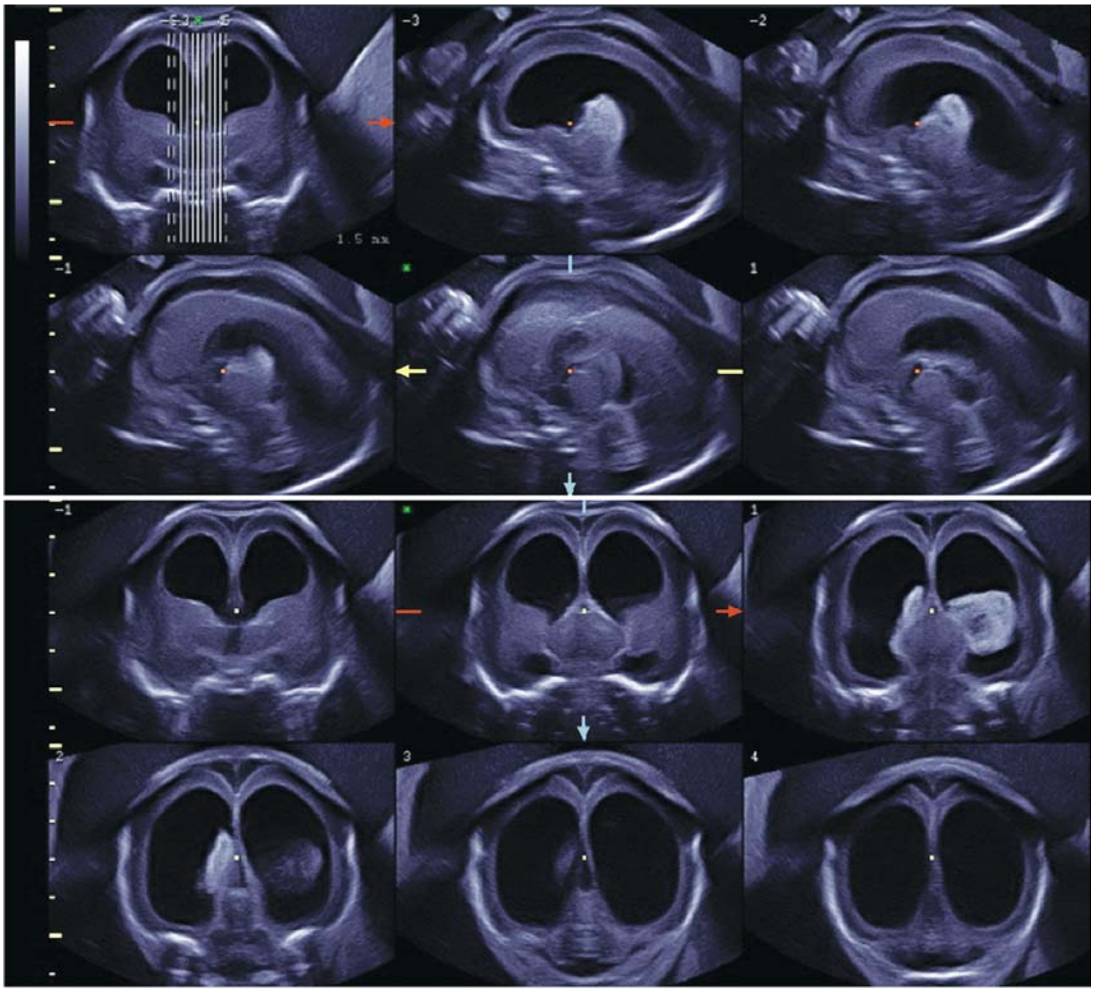

Fig. 12: Tomographic ultrasound images of hydrocephalus at 20 weeks of gestation. Upper: sagittal images; lower: coronal images

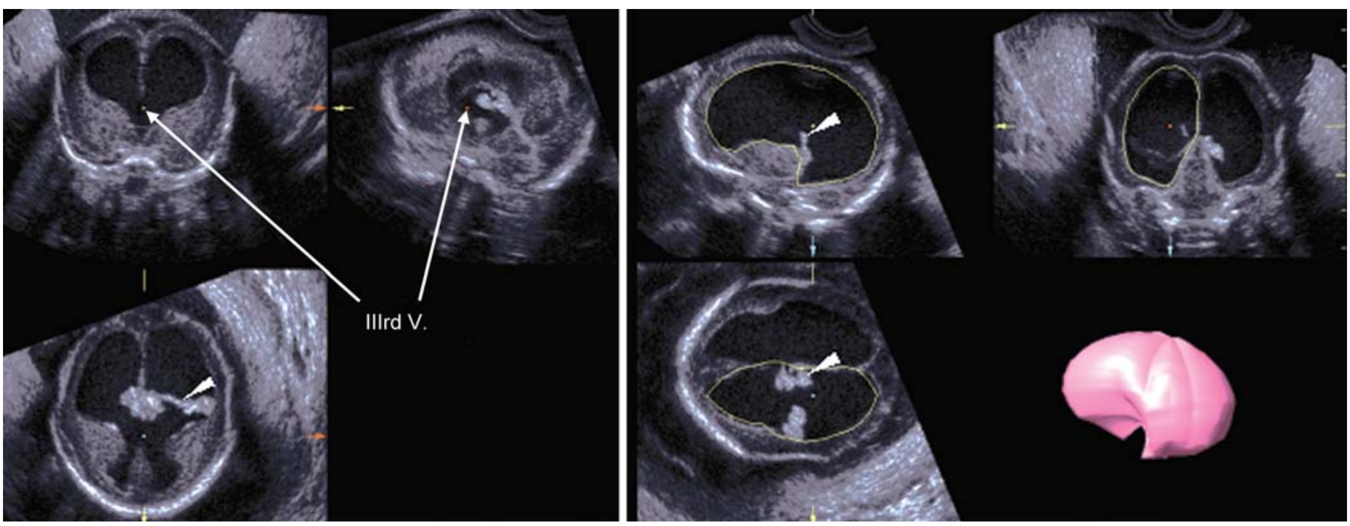

Fig. 13: Hydrocephalus due to aqueductal obstruction at 19 weeks of gestation. Left figure: Three orghogonal views with anterior coronal (upper left) and median sagittal (upper right) and axial (lower left) slices. Bilateral ventriculomegaly and third ventriculomegaly (IIIrd V.) are seen. No enlargement of fourth ventricle indicates obstruction of the aqueduct. Right figure: Three orghogonal views with parasagittal (upper left) and posterior coronal (upper right) and axial (lower left) slices. Subarachnoid space is already obliterated and dangling choroid plexus (arrowheads) is seen. Lower right pink figure shows extracted 3D ventricular image by VOCAL mode. Ventricle in this case was tenfold size of normal 19-week ventricle

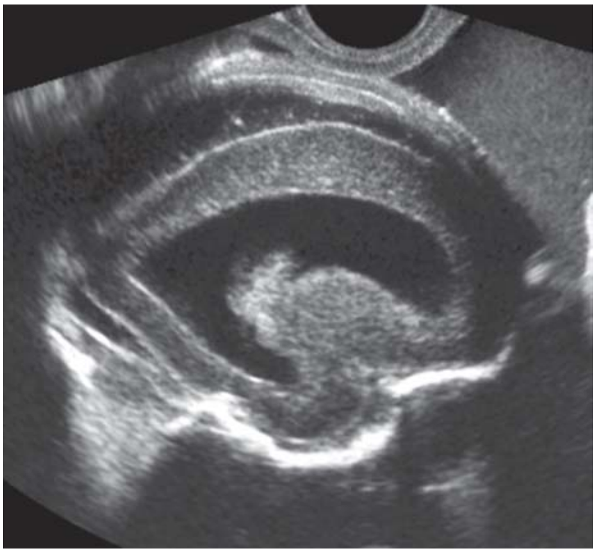

Fig. 14: US image of ventriculomegaly at 29 weeks of gestation. Enlarged ventricle exists but subarachnoid space is well preserved and no dangling choroid plexus is seen. From those findings, nonincreased intracranial pressure (ICP) is estimated. This condition should be differentiated from hydrocephalus with increased ICP

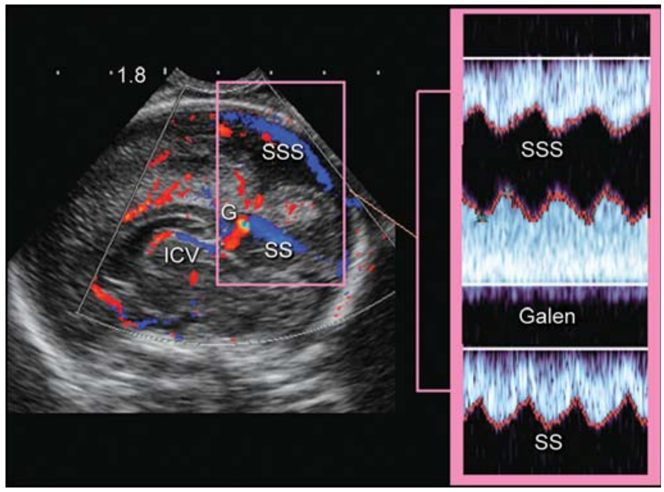

Fig. 15: Normal cerebral venous circulation. Left: sagittal image of color Doppler. SSS: superior sagittal sinus; ICV: internal cerebral vein; G: vein of Galen; SS: straight sinus; Right: normal blood flow waveforms of dural sinuses. In normal fetuses, venous flow always have pulsations

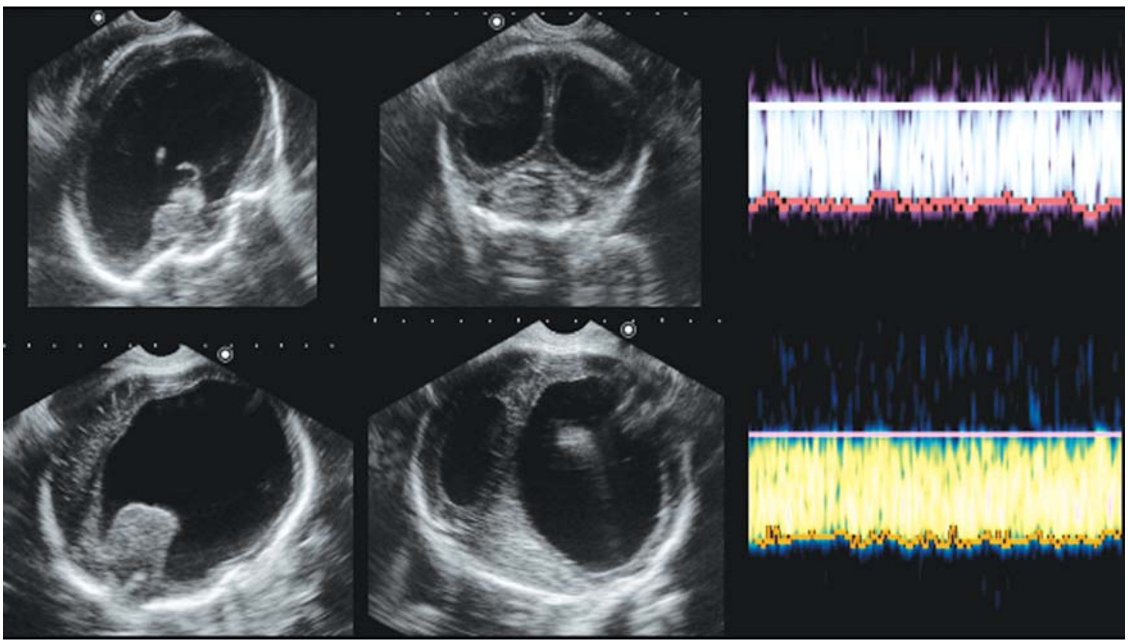

Fig. 16: Disappearance of venous pulsation in cases with hydrocephalus. Normal dural sinuses have pulsatile patterns of flow waveform (Fig. 26). In cases with progressive hydrocephalus, venous pulsation disappeared (right figures) may be because of excessive extension of the dura and dural sinuses

the bony defects (spina bifida occulta). The open spina bifida with protrusion of the spinal cord mainly occur in the lumbar, thoracolumbar or lumbosacral regions. Sonographic appearance of myelomeningocele is shown in Figures 20 and 21. Chiari type II malformation is present in almost every case of myelomeningocele. This malformation is characterized by inferior displacement of the lower cerebellum through the foramen magnum with obliteration of the cisterna magna (banana sign), inferior displacement of the medulla into the spinal canal, and deformity of the frontal bone with indentation (lemon sign). Both banana

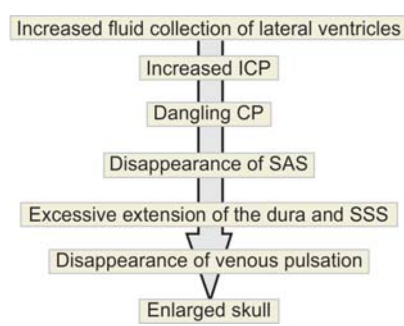

Fig. 17: Progressive stages of hydrocephalus. ICP: intracranial pressure; CP: choroid plexus; SAS: subarachnoid space; SSS: superior sagittal sinus

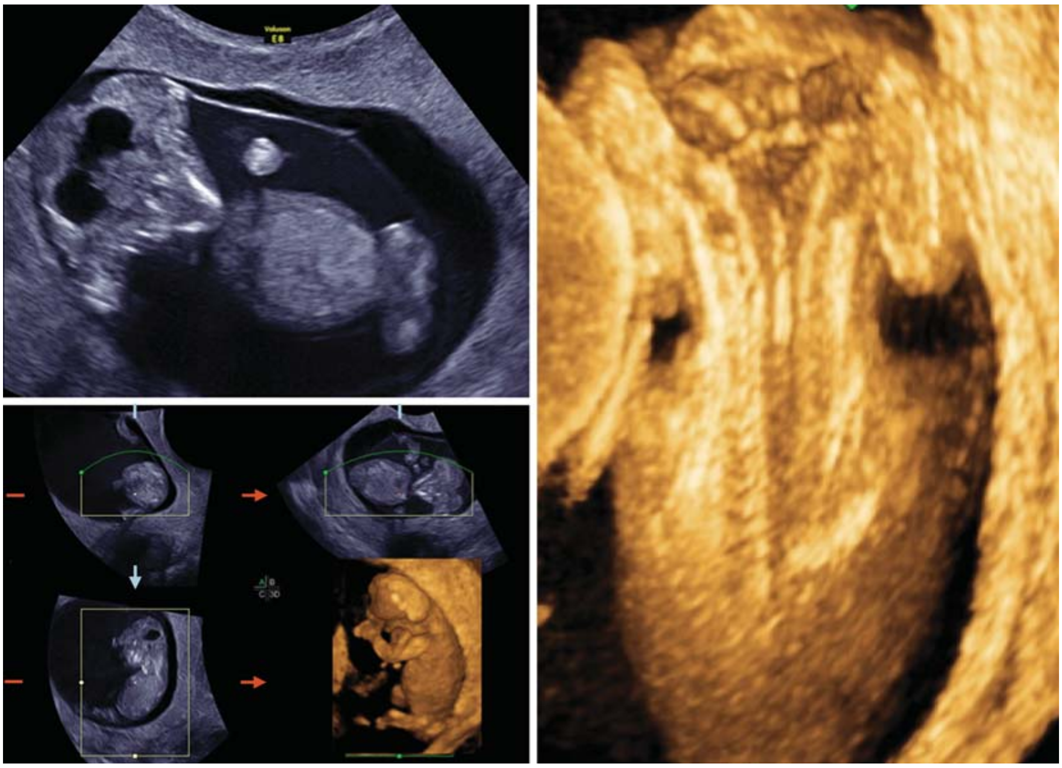

Fig. 18: Acrania at 11 weeks of gestation. Left upper: 2D coronal image. The normal appearance of amniotic membrane indicates no evidence of amniotic band syndrome. Right: 3D US occipital image of the same fetus

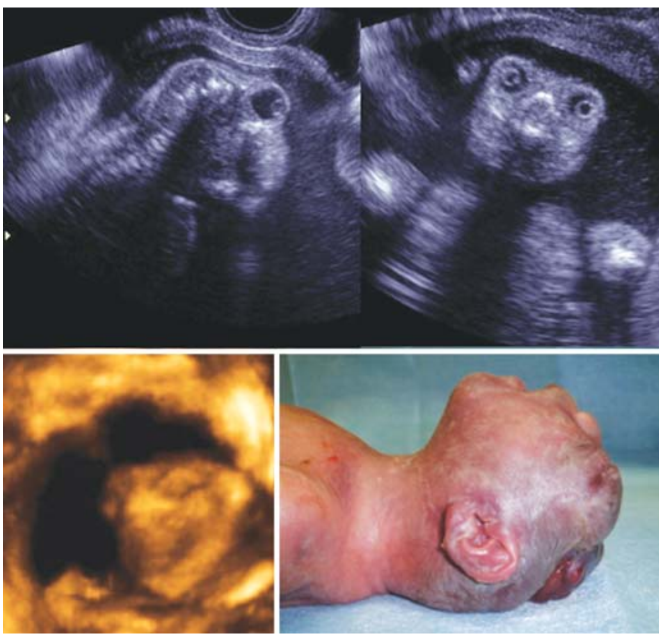

Fig. 19: Anencephaly in middle gestation (same case as Fig. 24). Upper left: US sagittal image at 23 weeks of gestation. Upper right: US coronal image. Lower left: 3D US image. Lower right: external appearances of stillborn fetus at 25 weeks of gestation. It is clear that excencephalic brain tissue scattered in the amniotic space compared with this case at 10 weeks

sign and lemon sign are detectable by sonography until 24 weeks' gestation (Fig. 22); and occasionally, the median section of craniovertebral junction demonstrates the medullary kink. Although the banana sign persists during pregnancy, the lemon sign may disappear in many cases with advancing gestational age.[30]

Disorders of Prosencephalic Development

Holoprosencephaly

Holoprosencephaly (Fig. 23) is caused by the disorder of prosencephalic development and is divided into the three subtypes: alobar, semilobar and lobar. Holoprosencephaly is frequently associated with other malformation, chromosomal aberration or Dandy-Walker malformation. A 75% of holoprosencephaly has normal karyotype, but chromosomes 2, 3, 7, 13, 18 and 21 have been implicated in holoprosencephaly. Particularly, trisomy 13 has most commonly been observed. The facial anomalies, such as cyclopia, cebocephaly, flatnose and cleft lip are often associated with holoprosencephaly. The characteristic appearance of fused ventricles is detectable from the early pregnancy.[31-33]

Agenesis of the Corpus Callosum

Agenesis of the corpus callosum [(complete agenesis, partial agenesis, dysgenesis, (Fig. 24)] leads abnormal induction of medial cerebral convolution. Agenesis of the corpus callosum is associated with additional cerebral anomalies, noncerebral anomalies and chromosomal aberration. It has been described that isolated agenesis of the corpus callosum *per se* has little consequence on neurological development. Gupta et al[34] reviewed 70 reported cases of agenesis of the

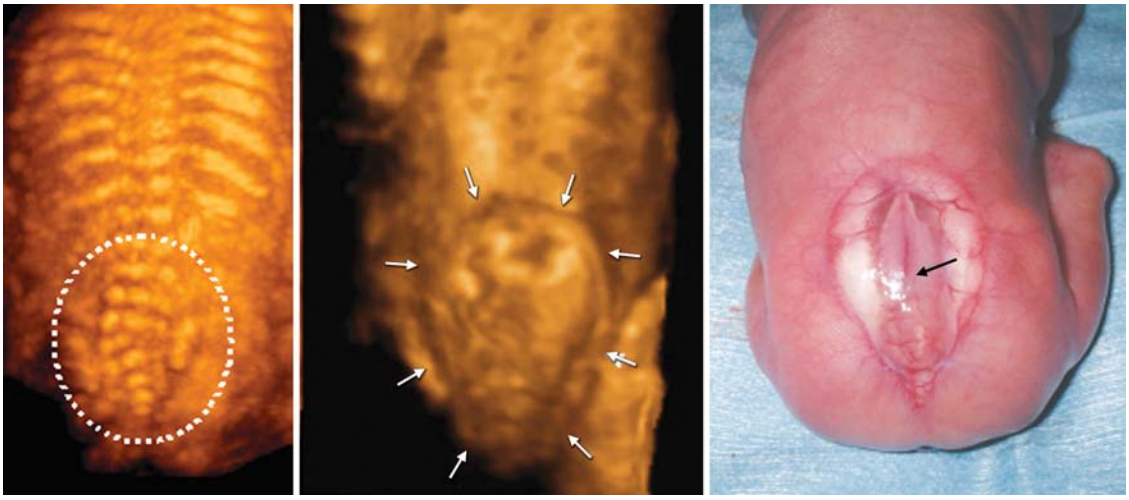

Fig. 20: Prenatal US image of myelomeningocele, spina bifida at 20 weeks of gestation. Left: 3D bony demonstration of lumber spina bifida. 3D ultrasound shows the exact level of spina bifida. Middle: 3D surface reconstruction of large myelomeningocele (white arrows). Right: external appearance of aborted fetus at 21 weeks of gestation. *Note*: The central canal of the spinal cord (black arrow) in large myelomeningocele

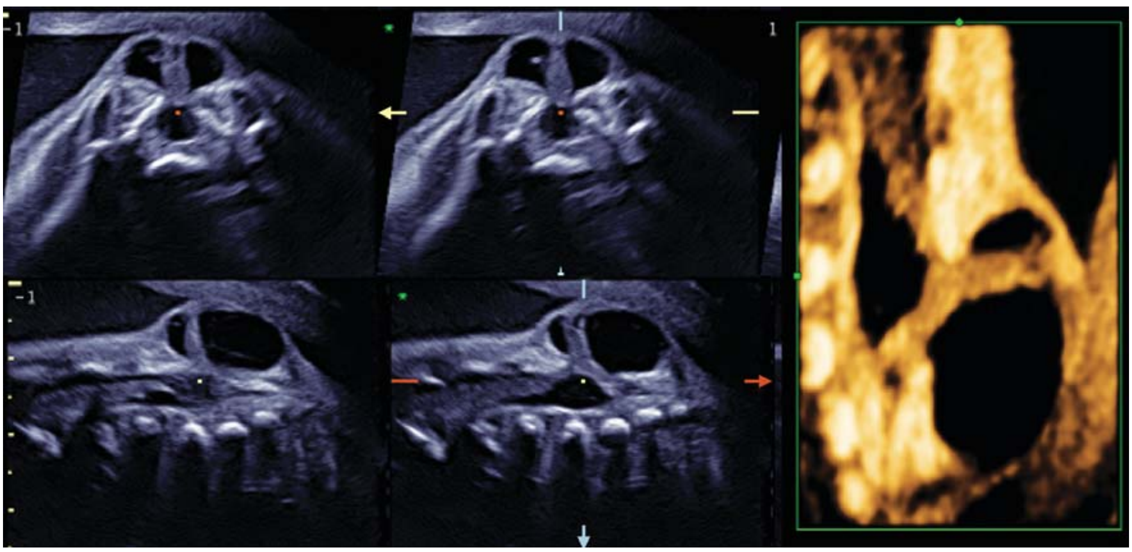

Fig. 21: 3D US tomographic images and 3D reconstructed image in a case of myelomeningocele at 26 weeks of gestation. Left upper: axial images; left lower: sagittal images; right: 3D image of spinal cord

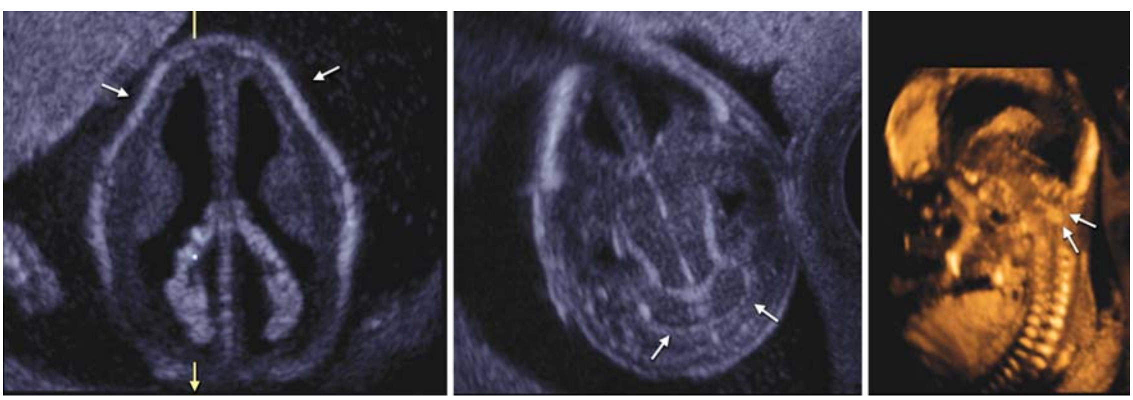

Fig. 22: Chiari type II malformation at 16 weeks of gestation. Chiari type II malformation is observed in most cases with myelomeningocele and myeloschisis. Left: typical lemon sign (arrows). Middle: typical banana sign (arrows). Right: 3D reconstruction internal image of Chiari type II malformation (arrows)

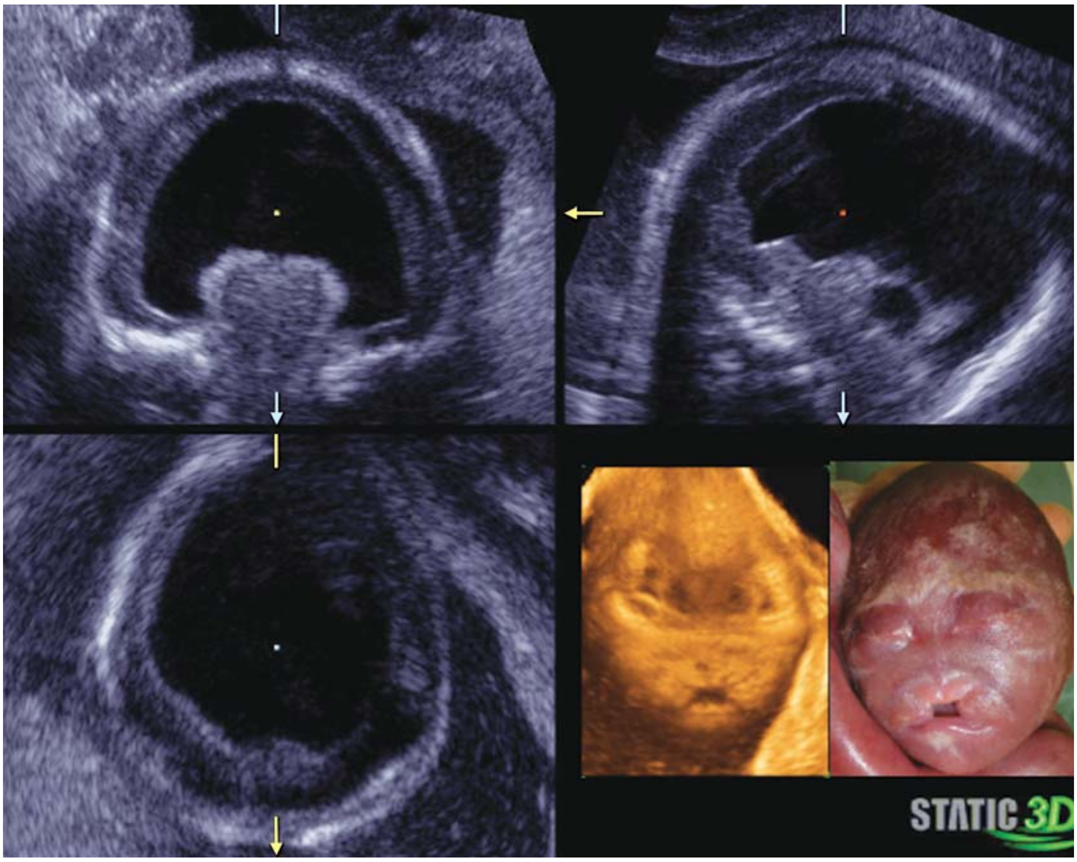

Fig. 23: Alobar holoprosencephaly at 20 weeks of gestation. Three orthogonal images of intracranial structure show complete single ventricle within a single-sphered cerebral structure. Lower right: 3D US image of fetal face and the face of aborted fetus at 21 weeks of gestation. A flat nose with median cleft lip/palate are seen

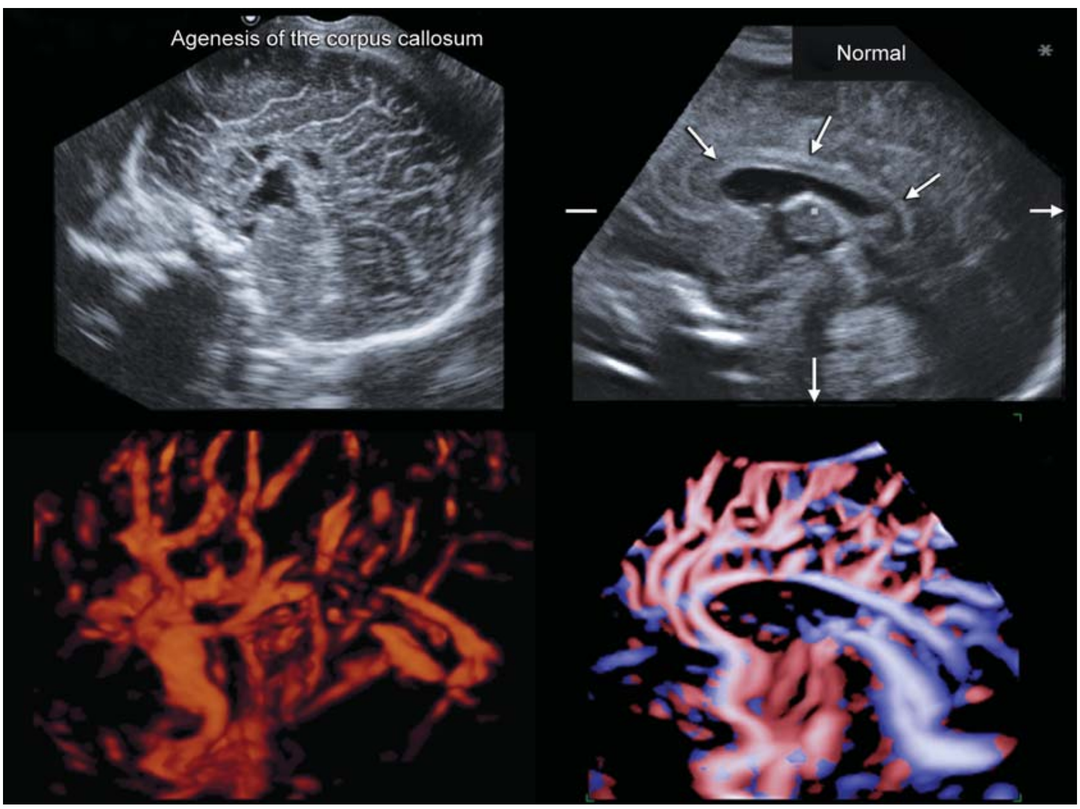

Fig. 24: Sagittal section of AOCC (agenesis of the corpus callosum, left) and normal case (right). Lower images are 3D power Doppler images of AOCC (left) and normal (right). Note the defect of callosomarginal artery in AOCC case

corpus callosum detected prenatally and described that 85% of fetuses without other detectable anomalies carried a normal development and 15% had a risk of handicap. Therefore, prenatal findings suggestive of agenesis of the corpus callosum should be followed by a careful search for associated anomalies and counseling parents should be prudent, if agenesis of the corpus callosum is an isolated finding. The typical findings of agenesis of the corpus callosum are the medial cerebral sulci demonstrated as a radial arrangement, enlargement of the posterior horns of lateral ventricles, steer-horn appearance of the anterior horns and upward displacement of the third ventricle. In most cases, detected prenatally by sonography, diagnosis was made by detection of indirect findings. The transvaginal median section of the brain, however, may be most reasonable to directly document the callosal lesion.

Migration Disorder

Lissencephaly

Lissencephaly is characterized by a lack of gyral development and divided into two types: type I has microcephaly and facial dysmorphism and often associated with Miller-Dierker syndrome and type II has hydrocephalus, retinal dysplasia and muscular dysplasia, associated with Walker-Warburg syndrome and Fukuyama congenital muscular dystrophy. Antenatal diagnosis of syndromes associated with lissencephaly before gyral development in families with prior affected infants has been reported by demonstration of additional abnormalities such as bilateral cataract[35] and hydrocephalus.[36] Sonographic detection of smooth gyral pattern at 31 to 32 weeks' gestation has been reported.[37] Prenatal sonographic diagnosis of lissencephaly, however, without a previous history cannot be reliably made until 26 to 28 weeks' gestation, when the normal gyri and sulci become well defined.

Posterior Fossa Anomalies

Dandy-Walker Complex

Dandy-Walker complex is used to indicate a spectrum of anomalies of the posterior fossa. Classification of Dandy-Walker complex is as follows:

1. *Dandy-Walker malformation (Classic)*—enlarged posterior fossa, complete or partial agenesis of the cerebellar vermis, elevated tentorium.

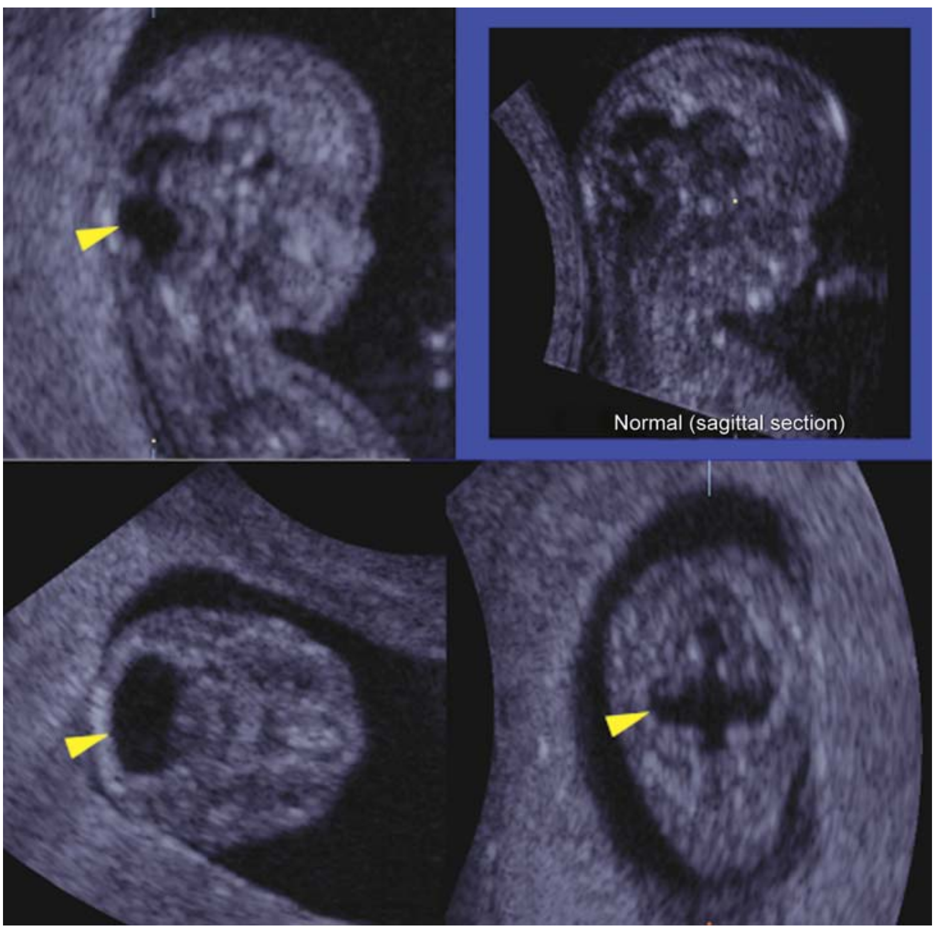

Fig. 25: Early stage of Dandy-Walker malformation at 11 weeks of gestation. Abnormal dilatation of the posterior fossa (arrowheads). Upper right figure is a sagittal image at the same gestational age in a normal case. Amniocentesis revealed trisomy 9 mosaicism and the fetus died *in utero* at 19 weeks

2. *Dandy-Walker variant*—variable hypoplasia of the cerebellar vermis with or without enlargement of the posterior fossa.
3. *Megacisterna magna*—enlarged cisterna magna with integrity of both cerebellar vermis and fourth ventricle.

Dandy-Walker malformation occurs as a part of recognizable syndromes such as Mechel's syndrome and Walker-Warburg syndrome, and is frequently associated with chromosomal aberrations. There often exist additional intracerebral or extracerebral anomalies. Congenital hydrocephalus exists in 5 to 10% of cases,[38] but hydrocephalus develops usually within 3 months after birth.[39] Antenatal diagnosis should be performed by a careful observation of the posterior fossa in the axial, coronal and sagittal planes. The closure of the cerebellar vermis in normal fetuses is demonstrated by sonography from 14 to 18 weeks' gestation. Bromley et al[37] described that 56% of normal fetuses had an open vermis at 14 weeks' gestation, 23% at 15 weeks and 6% at 17 weeks. Thus, the cerebellar vermis develops during early second trimester. The normal sonographic appearance of the open vermis should not be interpreted by developmental change of Dandy-Walker malformation and its variant, which is described as a small defect in the cerebellar vermis without dilatation of the cisterna magna. Prenatal diagnosis of Dandy-Walker variant should not be made before 18 weeks.[40] It was described that prenatal diagnosis of Dandy-Walker malformation is possible from 14 weeks' gestation.[41] Although early detection of Dandy-Walker complex should be done prudently, we had a case with Dandy-Walker malformation which was strongly suspected from 11 weeks of gestation (Fig. 25) because of abnormal dilatation of the posterior fossa.

Cerebellar Hypoplasia

Cerebellar dysplasia (Fig. 26) is often associated with chromosomal abnormalities such as trisomy 18 and others. In late pregnancy, prenatal diagnosis of cerebellar dysplasia is not difficult because of conspicuous enlargement of cisterna magna. However, in the first half of pregnancy, all normal cases have large cisterna magna. In order to detect cerebellar dysplasia, therefore, it is recommended to assess the development of the cerebellum measuring the cerebellar transverse diameter in axial image or posterior coronal section.

Other Disorders

Arachnoid Cyst

Arachnoid cyst (Fig. 27) is a congenital or acquired cyst, lined by arachnoid membranes, and filled with fluid collection which is the same character as the cerebrospinal fluid. The number of cysts is mostly single, but two or more cysts can be occasionally observed. Location of arachnoid cyst is various; approximately 50% of cysts occur from the Sylvian fissure (middle fossa). Interhemispheric cysts are often associated with agenesis or hypogenesis of the corpus callosum. Postnatal prognosis is usually good.

Choroid Plexus Cyst

Choroid plexus cysts are defined as cysts with fluid collection within the choroid plexus with incidence of 0.95 to 2.8% of all fetuses scanned,[42-44] which may exist unilaterally or bilaterally, associated with chromosomal

Fig. 26: Cerebellar dysplasia (28 weeks of gestation). Upper left: transvaginal median image. Small cerebellum in a normal size of posterior fossa. Upper right: transabdominal axial image. Lower left: fetal MR sagittal image. Lower right: MR axial image. This case has chromosomal aberration of trisomy 18 with other congenital anomalies such as large VSD, overlapping finger, lowset ears, etc.

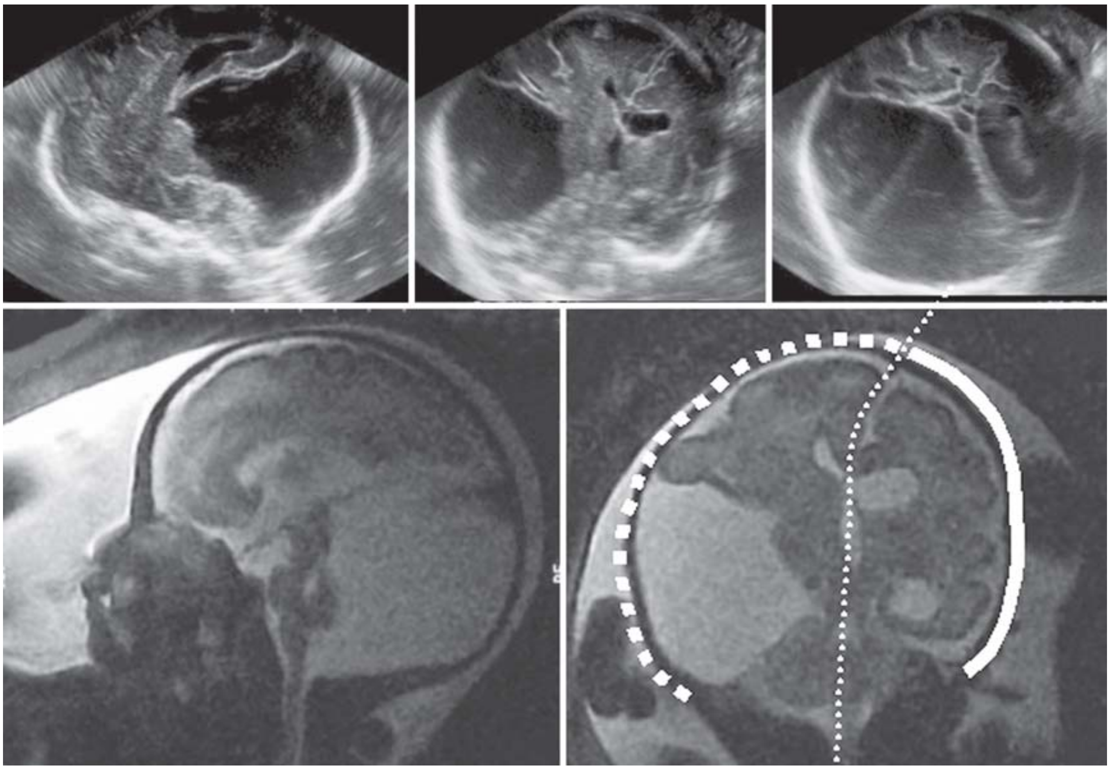

Fig. 27: Fetal arachnoid cyst at 31 weeks of gestation. Upper: transvaginal US image. Sagittal (left) and coronal (middle, right) sections. Lower left: fetal MR sagittal image. The cyst occupies supra- to infratentorial space. Not only cerebrum but also cerebellum are compressed by the cyst. Lower right: fetal MR coronal image. Midline is conspicuously arcuated. Scalp and skull bone are extended due to the existence of the huge cyst. *Note*: The difference between right and left head size

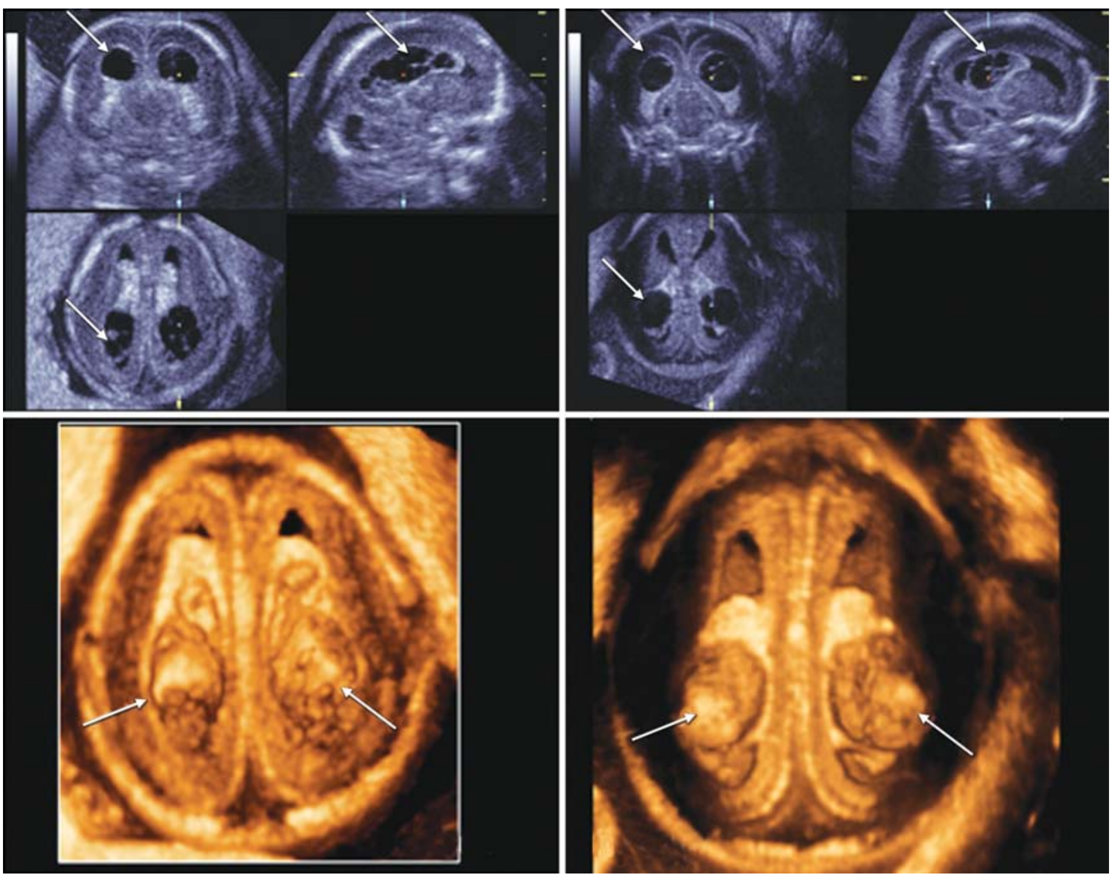

Fig. 28: Choroid plexus cysts (CPC) in cases of trisomy 18 (left) and normal karyotype (right). Left figures: three orthogonal views and inside 3D view of CPC in a case of trisomy 18 at 17 weeks of gestation. Various additional anomalies were detected. Right figures: three orhtogonal views and inside 3D view of CPC in a case with normal karyotype at 16 weeks. No additional abnormalities. Normal postnatal course. Impossible to differentiate normal from abnormal karyotypes only by location and appearance of choroid plexus cyst. Detection of additional anomalies is important for differentiated diagnosis

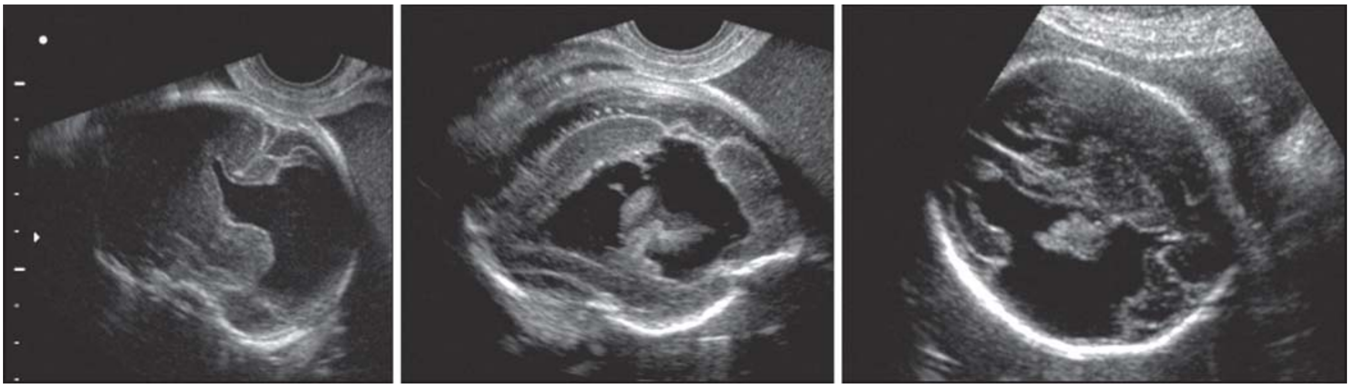

Fig. 29: Porencephaly at 25 weeks of gestation. Upper left: transvaginal US coronal image. Defect of parietolateral part of the unilateral cerebrum. This case has also absent septum pellucidum. Upper middle: parasagittal US image. Porencephalic part connects to unilateral ventricle. Echogenicity of inside ventricular wall indicates intraventricular hemorrhage. Upper right: transabdominal US axial image

aberration such as trisomy 18. They are depicted in the second trimester and usually spontaneous resolution is observed by the 24th week. Choroid plexus cysts per se are usually asymptomatic and benign, but rarely, symptomatic and disturb CSF flow.[45,46] It is impossible to differentiate normal from abnormal karyotypes only by location and appearance of choroid plexus cyst (Fig. 28). Isolated choroid plexus cysts may be normal variation. Fetal chromosomal examination should be offered if additional abnormalities are found.

Acquired Brain Abnormalities *in utero*

Intracranial Hemorrhage

Intracranial hemorrhage *in utero* may be caused by trauma, infections, asphyxia, alloimmune thrombocytopenia, intracranial tumor, cord complication, pre-eclampsia, abruptio placenta and other factors. Hemorrhage is commonly located in the subdural, periventricular and cerebellar regions. Many cases of intracranial hemorrhage detected prenatally have been reported.[47-52] The outcome of fetuses with intracranial hemorrhage has ranged from fetal demise and postnatal death to a good outcome with normal development.[48]

Porencephaly

Porencephaly [(porencephalic cyst, (Fig. 29)] is fluid-filled space replacing normal brain parenchyma and may or may not communicate with the lateral ventricles or subarachnoid space. Ischemic episode, trauma, demise of one twin, intercerebral hemorrhage, infection can cause porencephaly. It is easy to occur when immature cerebrum has some factors with propensity of dissolution and cavitation. Timing of ischemic injury (may be as early as second trimester) is strongly related to porencephaly.

FUTURE ASPECTS

The assessment of the fetal CNS plays an important role for the rest of infant's life. Advanced sonography combined with methodology of approaching the fetal brain has improved the assessment of fetal intracranial structure and diagnosis of the prenatal brain abnormalities. Recent remarkable development of three-dimensional/four-dimensional ultrasound and advanced MRI technology[53-55] will produce more accurate evaluation of the brain morphology. A functional evaluation of the intracranial condition and a prenatal prediction of neurological development after birth are also important points in a proper management for fetuses with intracranial abnormalities, but many uncertain and unknown facts still exist. Further studies on the assessment of cerebral function may be expected.

REFERENCES

1. The nervous system. In Moore KL, Persaud TVN, Shiota K, editors: Color Atlas of Clinical Embryology. Philadelphia, USA: WB Saunders 1994;209-220.
2. Timor-Tritsch IE, Peisner DB, Raju S. Sonoembryology: an organ-oriented approach using a high-frequency vaginal probe. J Clin Ultrasound 1990;18:286-298.
3. Pooh RK. B-mode and Doppler studies of the abnormal fetus in the first trimester. In Chervenak FA, Kurjak A, editors: Fetal Medicine. Carnforth: Parthenon Publishing, 1999;46-51.
4. Timor-Tritsch IE, Monteagudo A. Transvaginal fetal neurosonography: standardization of the planes and sections by anatomic landmarks. Ultrasound Obstet Gynecol 1996;8:42-47.
5. Monteagudo A, Reuss ML, Timor-Tritsch IE. Imaging the fetal brain in the second and third trimesters using transvaginal sonography. Obstet Gynecol 1991;77:27-32.
6. Monteagudo A, Timor-Tritsch IE, Moomjy M. In utero detection of ventriculomegaly during the second and third trimesters by transvaginal sonography. Ultrasound Obstet Gynecol 1994;4:193-198.
7. Monteagudo A, Timor-Tritsch IE. Development of fetal gyri, sulci and fissures: a transvaginal sonographic study. Ultrasound Obstet Gynecol 1997;9:222-228.

8. Pooh RK, Nakagawa Y, Nagamachi N, et al. Transvaginal sonography of the fetal brain: detection of abnormal morphology and circulation. Croat Med J 1998;39:147-157.
9. Pooh RK, Maeda K, Pooh KH, Kurjak A. Sonographic assessment of the fetal brain morphology. Prenat Neonat Med 1999;4:18-38.
10. Pilu G, Falco P, Milano V, Perolo A, Bovicelli L. Prenatal diagnosis of microcephaly assisted by vaginal sonography and power Doppler. Ultrasound Obstet Gynecol 1998;11:357-360.
11. Pretorius DH, Nelson TR. Three-dimensional ultrasound. Ultrasound Obstet Gynecol 1995;5:219-221.
12. Merz E. Three-dimensional ultrasound—a requirement for prenatal diagnosis. Ultrasound Obstet Gynecol 1998;12:225-226.
13. Kurjak A, Kupesic S, Banovic I, Hafner T, Kos M. The study of morphology and circulation of early embryo by three-dimensional ultrasound and power Doppler. J Perinat Med 1999;27:145-157.
14. Pooh RK. Fetal brain assessment by three-dimensional ultrasound. In Kurjak A, Kupesic S, editors: Clinical application of 3D sonography. Carnforth: Parthenon Publishing, 2000; 171-179.
15. Pooh RK, Pooh K, Nakagawa Y, Nishida S, Ohno Y. Clinical application of three-dimensional ultrasound in fetal brain assessment. Croat Med J 2000;41:245-251.
16. Pooh RK. Neuroanatomy visualized by 2D and 3D. In: Pooh RK, Kurjak A, editors. Fetal neurology. Jaypee Brothers Medical Publishers, New Delhi 2009:15-38.
17. Timor-Tritsch IE, Monteagudo A, Mayberry P. Three-dimensional ultrasound evaluation of the fetal brain: the three horn view. Ultrasound Obstet Gynecol 2000;16:302-306.
18. Pooh RK, Pooh KH. Transvaginal 3D and Doppler ultrasonography of the fetal brain. Semin Perinat 2001;25: 38-43.
19. Pooh RK, Nagao Y, Pooh KH. Fetal neuroimaging by transvaginal 3D ultrasound and MRI. Ultrasound Rev Obstet Gynecol 2006;6:123-134.
20. Pooh RK, Kurjak A. 3D and 4D sonography and magnetic resonance in the assessment of normal and abnormal CNS development: alternative or complementary. J Perinat Med 2011:39(1):3-13.
21. Endres LK, Cohen L. Reliability and validity of three-dimensional fetal brain volumes. J Ultrasound Med 2001;20:1265-1269.
22. Roelfsema NM, Hop WC, Boito SM, Wladimiroff JW. Three-dimensional sonographic measurement of normal fetal brain volume during the second half of pregnancy. Am J Obstet Gynecol 2004;190:275-280.
23. Pooh RK, Pooh KH, Nakagawa Y, Maeda K, Fukui R, Aono T. Transvaginal Doppler assessment of fetal intracranial venous flow. Obstet Gynecol 1999;93:697-701.
24. Martinez de Villarreal L, Perez JZ, Vazquez PA, Herrera RH, Campos Mdel R, Lopez RA, et al. Decline of neural tube defects cases after a folic acid campaign in Nuevo Leon, Mexico. Teratology 2002;66:249-256.
25. Ray JG, Meier C, Vermeulen MJ, Boss S, Wyatt PR, Cole DE. Association of neural tube defects and folic acid food fortification in Canada. Lancet 2002;360:2047-2048.
26. Persad VL, van den Hof MC, Dube JM, Zimmer P. Incidence of open neural tube defects in Nova Scotia after folic acid fortification. CMAJ 2002;167:241-245.
27. Mathews TJ, Honein MA, Erickson JD. Spina bifida and anencephaly prevalence: United States, 1991-2001. MMWR Recomm Rep 2002;51:9-11.
28. Green NS. Folic acid supplementation and prevention of birth defects. J Nutr 2002;132:2356S-2360S.
29. Monteagudo A, Timor-Tritsch IE. Fetal neurosonography of congenital brain anomalies. In: Timor-Tritsch IE, Monteagudo A, Cohen HL, editors: ultrasonography of the Prenatal and Neonatal Brain. 2nd ed. New York: McGraw-Hill 2001; 151-258.
30. van den Hof MC, Nicolaides KH, Campbell J, Campbell S. Evaluation of the lemon and banana signs in one hundred thirty fetuses with open spina bifida. Am J Obstet Gynecol 1990;162:322-327.
31. Pilu G, Perolo A, David C. Midline anomalies of the brain. In Timor-Tritsch IE, Monteagudo A, Cohen HL, editors: Ultrasonography of the Prenatal and Neonatal Brain. Stamford, USA: Appleton and Lange 1996;241-258.
32. Bronshtein M, Weiner Z. Early transvaginal sonographic diagnosis of alober holoprosencephaly. Prenat Diagn 1991;11:459-462.
33. Gonzalez-Gomez F, Salamanca A, Padilla MC, Camara M, Sabatel RM. Alobar holoprosencephalic embryo detected via transvaginal sonography. Eur J Obstet Gynecol Reprod Biol 1991;47:266-270.
34. Gupta JK, Lilford RJ. Assessment and management of fetal agenesis of the corpus callosum. Prenat Diagn 1995;15: 301-312.
35. Bornemann A, Pfeiffer R, Beinder E, Wenkel H, Schlicker U, Meyermann R, et al. Three siblings with Walker-Warburg syndrome. Gen and Diagn Pathol 1997;141:371-375.
36. Gasser B, Lindner V, Dreyfus M, Feidt X, Leissner P, Treisser A, et al. Prenatal diagnosis of Walker-Warburg syndrome in three sibs. Am J Med Genet 1998;76:107-110.
37. Saltzman DH, Krauss CM, Goldman JM, Benacerraf BR. Prenatal diagnosis of lissencephaly. Prenat Diagn 1991;11: 139-143.
38. Volpe JJ. Neural tube formation and prosencephalic development. Neurology of the Newborn. Philadelphia, USA: WB Saunders 2001;3-42.
39. Hirsch JF, Pierre-Kahn A, Renier D, Sainte-Rose C, Hoppe-Hirsch E. The Dandy-Walker malformation: A review of 40 cases. J Neurosurg 1984;61:515-522.
40. Blomley B, Nadel AS, Pauker S, Estroff JA, Benacerraf BR. Closure of the cerebellar vermis: Evaluation with second trimester US. Radiology 1994;193:761-763.
41. Ulm B, Ulm MR, Deutinger J, Bernaschek G. Dandy-Walker malformation diagnosed before 21 weeks of gestation: associated malformation and chromosomal abnormalities. Ultrasound Obstet Gynecol 1997;10:167-170.
42. Sullivan A, Giudice T, Vavelidis F, Thiagarajah S. Choroid plexus cysts: is biochemical testing a valuable adjunct to targeted ultrasonography? Am J Obstet Gynecol 1999;181:260-265.
43. Reinsch RC. Choroid plexus cysts-association with trisomy: Prospective review of 16,059 patients. Am J Obstet Gynecol 1997;176:1381-1383.
44. Morcos CL, Platt LD, Carlson DE, Gregory KD, Greene NH, Korst LM. The isolated choroid plexus cyst. Obstet Gynecol 1998;92: 232-236.

45. Lam AH, Villanueva AC. Symptomatic third ventricular choroid plexus cysts. Pediatr Radiol 1992;22(6):413-416.
46. Parizek J, Jakubec J, Hobza V, Nemeckova J, Cernoch Z, Sercl M, et al. Choroid plexus cyst of the left lateral ventricle with intermittent blockage of the foramen of Monro, and initial invagination into the III ventricle in a child. Childs Nerv Syst 1998;14:700-708.
47. Forgaty K, Cohen HL, Haller JO. Sonography of fetal intracranial hemorrhage: Unusual causes and a review of the literature. J Clin Ultrasound 1989;17:366-370.
48. Achiron R, Pinchas OH, Reichman B, Heyman Z, Schimmel M, Eidelman A, et al. Fetal intracranial haemorrhage: clinical significance of in utero ultrasonographic diagnosis. Br J Obstet Gynaecol 1993;100:995-999.
49. Anderson MW, McGahan JP. Sonographic detection of an in utero intracranial hemorrhage in the second trimester. J Ultrasound Med 1994;13:315-318.
50. Catenzarite VA, Schrimmer DB, Maida C, Mendoza A. Prenatal sonographic diagnosis of intracranial hemorrhage: Report of a case with a sinusoidal fetal heart rate tracing and review of the literature. Prenat Diagn 1995;15:229-235.
51. Reiss I, Gortner L, Mller J, Gehl HB, Baschat AA, Gembruch U. Fetal intracerebral hemorrhage in the second trimester: diagnosis by sonography and magnetic resonance imaging. Ultrasound Obstet Gynecol 1996;7:49-51.
52. Guerriero S, Ajossa S, Mais V, Risalvato A, Angiolucci M, Labate F, et al. Color Doppler energy imaging in the diagnosis of fetal intracranial hemorrhage in the second trimester. Ultrasound Obstet Gynecol 1997;10:205-208.
53. Pooh RK, Pooh KH. The assessment of fetal brain morphology and circulation by transvaginal 3D sonography and power Doppler. J Perinat Med 2002;30:48-56.
54. Pooh RK, Pooh KH. Fetal neuroimaging with new technology. Ultrasound Review Obstet Gynecology 2002;2:178-181.
55. Pooh RK, Maeda K, Pooh KH. An atlas of fetal central nervous system disease: diagnosis and management. Parthenon CRC Press: London, New York, 2003.

ABOUT THE AUTHORS

Ritsuko K Pooh (Corresponding Author)

Director, Fetal Diagnosis Unit, CRIFM Clinical Research Institute of Fetal Medicine PMC, 7-3-7 Uehommachi, Tennoji, Osaka #543-0001, Japan, Phone: +81-6-6775-8111, Fax: +81-6-6775-8122 e-mail: evp-pooh@fetal-medicine-pooh.jp

KyongHon Pooh

Director, Department of Neurosurgery, Shikoku Medical Center for Children and Adults, 2-1-1, Senyucho, Zentsuji, Kagawa, Japan